

# Ellipsometry noise spectrum, suspension transfer function measurement and closed-loop control of the suspension system in the Q & A experiment

Sheng-Jui Chen\*, Hsien-Hao Mei and Wei-Tou Ni

Center for Gravitation and Cosmology, Department of Physics,  
National Tsing Hua University, Hsinchu, Taiwan 30055, Republic of China

**Abstract.** The Q & A experiment, aiming at the detection of vacuum birefringence predicted by quantum electrodynamics, consists mainly of a suspended 3.5 m Fabry-Perot cavity, a rotating permanent dipole magnet and an ellipsometer. The 2.3 T magnet can rotate up to 10 *rev/s*, introducing an ellipticity signal at twice the rotation frequency. The X-pendulum gives a good isolation ratio for seismic noise above its main resonant frequency 0.3 Hz. At present, the ellipsometry noise decreases with frequency, from  $1 \times 10^{-5}$   $\text{rad}\cdot\text{Hz}^{-1/2}$  at 5 Hz,  $2 \times 10^{-6}$   $\text{rad}\cdot\text{Hz}^{-1/2}$  at 20 Hz to  $5 \times 10^{-7}$   $\text{rad}\cdot\text{Hz}^{-1/2}$  at 40 Hz. The shape of the noise spectrum indicates possible improvement when the movement between the cavity mirrors is further controlled and reduced. From the preliminary result of yaw motion alignment control, it can be seen that some peaks due to yaw motion of the cavity mirror was suppressed. In this paper, we first give a schematic view of the Q & A experiment, and then present the measurement of transfer function of the compound X-pendulum-double pendulum suspension. A closed-loop control was carried out to verify the validity of the measured transfer function. The ellipsometry noise spectra with and without yaw alignment control and the newest improvement is presented.

\*E-mail: d883374@oz.nthu.edu.tw

PACS numbers: 04.80.-y, 12.20.-m, 14.80.Mz, 07.60.Ly, 07.60.Fs, 33.55.Ad

## 1. Introduction

Quantum Electrodynamics (QED) predicts that vacuum is birefringent under the influence of a strong magnetic field [1-6]. For a B field of 2.5 T, the difference of index of refraction experienced by the light with polarization parallel and with polarization perpendicular to the B field is  $\Delta n \equiv n_{\parallel} - n_{\perp} = 2.5 \times 10^{-23}$ . This tiny effect can be detected by a precision determination of the induced ellipticity on a laser beam [5]. The development of ultrahigh-precision technology in the laser-interferometric gravitational-wave detection community prompted our thought of its application to this matter [6]. First experiment was done in 1993 by Cameron *et al* [7] with good upper bounds on vacuum birefringence and polarization rotation. A pseudo-scalar interaction with electromagnetism ( $\mathcal{L}_I \sim F_{ij} F_{kl} e^{ijkl}$ ) was proposed which was empirically allowed in the study of equivalence principles [8-10]; in terms of Feynman diagram, this interaction gives a 2-photon-pseudo-scalar vertex. With this interaction, vacuum becomes birefringent and dichroic [11-13]. In 1994, 3 experiments were put forward and started for measuring the vacuum birefringence: the PVLAS experiment

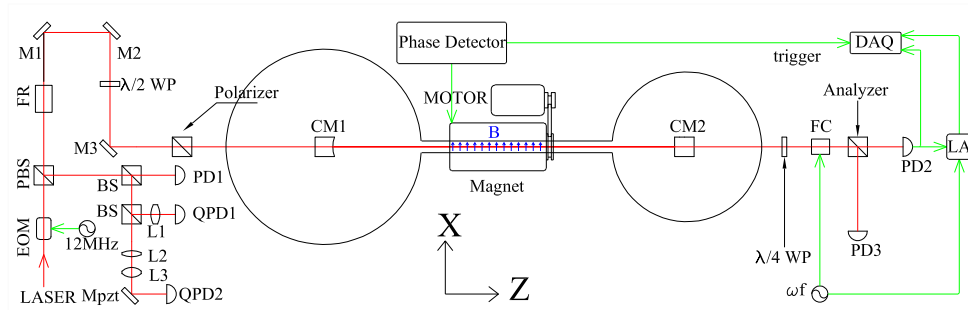


**Figure 1.** Experimental Setup. EOM electro-optical modulator;  $\lambda/2$  WP half-wave plate;  $\lambda/4$  WP quarter-wave plate; L1, L2, L3 lenses; M1, M2, M3 steering mirrors; PBS polarizing beam splitter; Mpzt Piezo-driven steering mirror; BS beam splitter; FR Faraday rotator; CM1, CM2 cavity mirrors; B magnetic field; PD1, PD2, PD3 photo-receivers; QPD1, QPD2 quadrant photodiodes ; FC Faraday cell; DAQ data acquisition system; LA lock-in amplifier.

[14], the Fermilab P-877 experiment [15], and the Q & A (QED & Axion) experiment [16]; these experiments were reported in the "Frontier Test of QED and Physics of Vacuum" Meeting in 1998. Fermilab P-877 experiment was terminated in 2000. This year in the QED-2005 (QED, Quantum Vacuum and the Search for New Forces, Les Houches, France, June, 2005) conference, again, 3 experiments were reported: the PVLAS experiment [17], the BMV experiment [18], and the Q & A experiment [19]. A compilation of basic characteristics of these 3 experiments were given in [20]. All 3 experiments use a high-finesse Fabry-Perot Interferometer (FPI) cavity to enhance the effect to be measured. The PVLAS experiment reported a positive measurement of polarization rotation and suggested a possible interpretation of this result to the existence of a pseudoscalar particle coupled to photons [17, 21].

In 2002, we had constructed and tested our prototype 3.5 m high-finesse Fabry-Perot interferometer (FPI) with ellipsometry [22]. Since then, we have been making efforts to improve the stability of feedback control and the sensitivity of ellipticity detection. Figure 1 shows the experimental setup. The laser beam is phase modulated at 12 MHz for Pound-Drever-Hall locking technique. Before entering the FPI, the laser is linearly polarized by a polarizing prism of Glan-Taylor type with an extinction ratio around 90 dB. Each mirror of the FPI is suspended by an X-pendulum [23] with a double pendulum as the second stage, as shown in figure 2. X-pendulum was designed and developed by the TAMA group, a two-dimensional horizontal low frequency vibration isolator. We followed their design closely and obtained a resonant frequency of 0.3 Hz. The double pendulum consists of an intermediate mass IM, a recoil mass RM and the mirror CM1. The longitudinal length of the FPI can be adjusted by applying force to magnets on the CM1 through coils held by the RM. A 0.6 m long rotating permanent dipole magnet with a maximum central field of 2.3 T is located between CM1 and CM2 for producing a polarized vacuum that is to be probed by the laser beam resonating inside the FPI. After the laser leaving out of FPI, the induced ellipticity on it is transformed into polarization rotation by a  $\lambda/4$  wave-plate for frequency mixing with the modulation provided by the Faraday cell FC

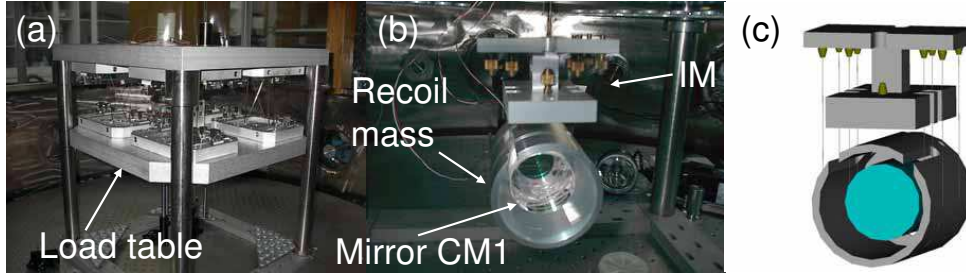


**Figure 2.** (a) Picture of the X-pendulum (b) Picture of the double pendulum (c) CAD drawing of the double pendulum.

[7]. Finally, the laser is extinguished by another polarizing prism whose transmission axis is aligned orthogonally to the polarizer's transmission axis. The transmitted light and reflected light are received by PD2 and PD3 respectively. The output of PD3 is used for switching on/off the feedback force on CM1. PD1, QPD1 and QPD2 are the essential sensors for maintaining the FPI at its working point. In the following, we present the transfer function measurement, feedback control and the preliminary results. Outlook and discussion is given in the end.

## 2. Transfer function measurement

For active control of the cavity mirror, we have measured the transfer function (TF) from the coil-magnet pair actuators to the displacement and rotation of the cavity mirror. An HP 3-axis heterodyne interferometer capable of sensing two rotational and one longitudinal motions of the cavity mirror was used as the sensor. The cavity mirror and the IM were arranged in a double pendulum configuration and suspended from the load table of the X-pendulum. Coils were held by a rigid frame extended from the load table of the X-pendulum. Because the mass of the load table is much larger than that of the cavity mirror, the transfer function was reduced to a double pendulum's TF. One of the measured transfer functions is shown in figure 3. A closed-loop control was performed to verify the measured TFs. The loop filter was designed and optimized by the closed-loop simulation with the model TF, and realized by a digital control unit. In figure 4, the rms amplitude was suppressed from  $4.05 \mu\text{m}$  to  $0.23 \mu\text{m}$  for the longitudinal motion and from  $15.5 \mu\text{rad}$  to  $4.4 \mu\text{rad}$  for the yaw motion. In this test, we found that when the load table of the X-pendulum was excited by the environment, the control became unstable. It was possibly due to the presence of the X-pendulum's resonance which leads to an extra pole appearing in the TFs. To overcome it, the double pendulum has been modified as it is in figure 2. Coils are held by a weight-matched (to CM1) recoil mass, the TF for the longitudinal motion is reduced to that of a simple pendulum. This allows a wider bandwidth and a better stability in control. The TF for yaw is still characterized by a model TF as in figure 3, for the moment-of-inertia is not matched in this design.

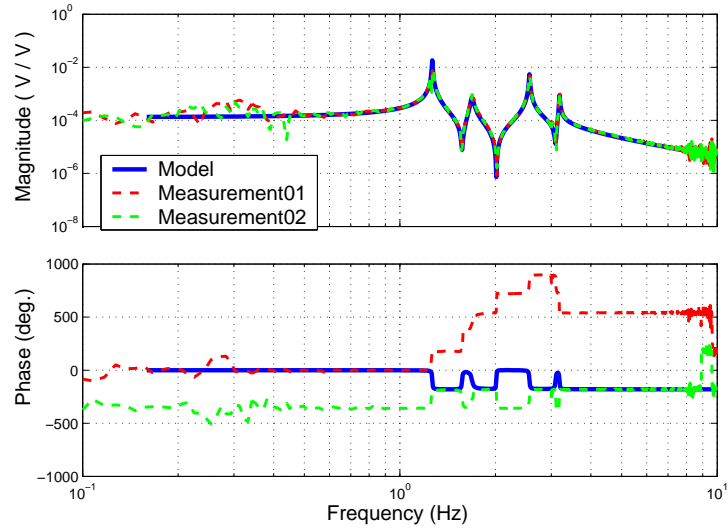


Figure 3. The yaw (rotation along the vertical axis) transfer function.

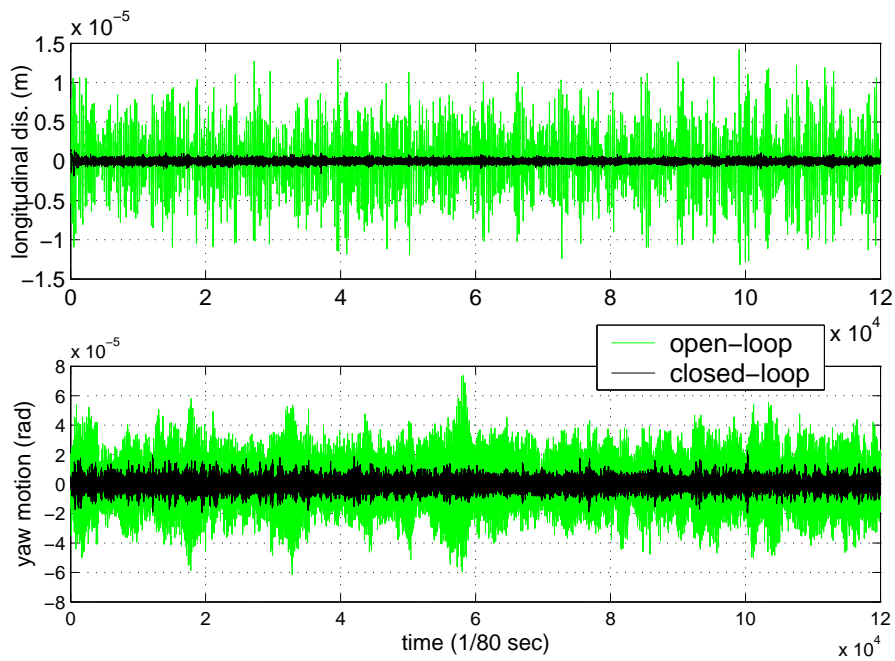


Figure 4. Open-loop vs. closed-loop control longitudinal displacement and yaw motion.

### 3. Feedback control

#### 3.1. Longitudinal control

Because of the large resonant displacement of the X-pendulum, the frequency range of the laser is not sufficient to track the cavity resonant frequency. Thus, the error signal for longitudinal control has to be fed back into two paths: one for frequency of the laser with a dynamic range of  $\pm 120$  MHz and a bandwidth over 100 kHz; another one for cavity length control with a dynamic range of  $\pm 3$  mm ( $\sim \pm 240$  GHz) and a bandwidth of about 200 Hz. In the first path, a typical loop filter consisting of an integrator and a lag compensator was used; in the second path, the loop filter was a first-order low pass filter whose cut-off frequency is 100 Hz in series with a lag compensator. The ratio of DC gains of these two paths determines the stability of the closed-loop control. The unit gain frequency of the longitudinal open-loop TF is 13.3 kHz.

#### 3.2. Alignment control

The differential wavefront sensing technique [24] is adopted here. We use a quadrant photodiode (QPD) with a resonant circuit [25] as our wavefront sensor. An active control on centering the interference pattern on the QPD was employed for reducing spurious alignment signal. The bandwidth for the yaw alignment control was about 15 Hz and the loop filter basically consisted of an integrator and a bi-quadratic filter (a complex zero and a complex pole). The transient response while closing the yaw alignment control loop is plotted in figure 5. The longitudinal loop acquired the "lock" at time = 0 s from an "off-lock" event. Some yaw motion excited by the event remained and can not be suppressed by the longitudinal loop. At time = 34 s, the yaw alignment control was turned on and began to rotate the mirror to its proper orientation and to stop the mirror's yaw motion. The consequence is that the transmitted light power increased and its fluctuation decreased. The effect of the yaw alignment control can also be seen in the ellipticity noise spectrum in figure 6. Now, only one out of four degrees of freedom of cavity mirrors is actively controlled. The three remaining d.o.f.'s will be controlled soon after this conference.

### 4. Preliminary results

The sensitivity curve of ellipticity detection by now is plotted in figure 6. The signal current  $I$  received by PD2 in figure 1 can be described by the Malus law  $I = I_0[\sigma^2 + (\alpha + \eta_0 \cos \omega_f t)^2]$  where  $I_0$  is the signal when the analyzer is rotated for maximum transmission of analyzed light,  $\sigma^2$  is the extinction ratio of the analyzer,  $\alpha$  is the ellipticity signal coming from various noise sources and  $\eta_0 \cos \omega_f t$  is the modulation of polarization rotation with a modulation depth of  $\eta_0$  at frequency  $\omega_f$ . After demodulation,  $\alpha$  was obtained. In the spectrum of  $\alpha$ , the noise density decreases with frequency, from  $1 \times 10^{-5}$  rad·Hz $^{-1/2}$  at 5 Hz,  $2 \times 10^{-6}$  rad·Hz $^{-1/2}$  at 20 Hz to  $5 \times 10^{-7}$  rad·Hz $^{-1/2}$  at 40 Hz. From the shape of the spectrum, we can infer that part of the noise comes from the noisy motion of the cavity mirror. This is more evident when the yaw alignment control was turned on. The dashed line in figure 6 is lower than the solid one for frequency below 15 Hz. But above 15 Hz, extra noise was introduced by the alignment control. We are still working on this, to find out where the noise is from and to eliminate it.

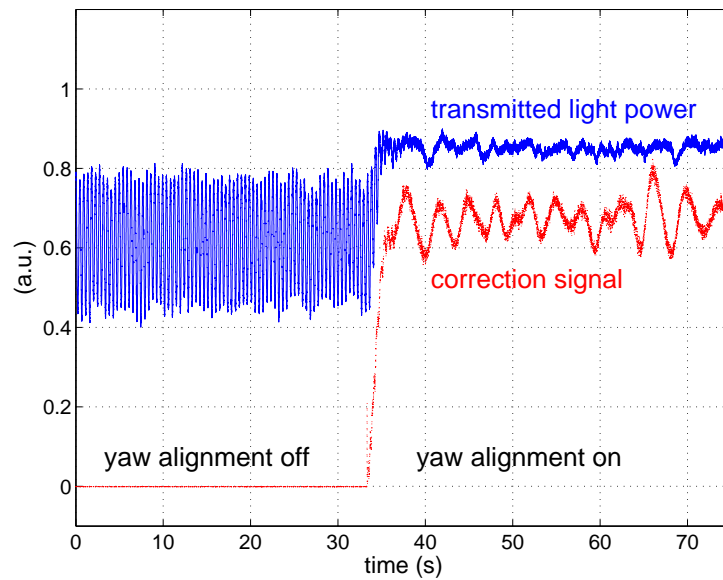


**Figure 5.** The lower curve is the correction signal on the yaw motion actuator. When the control is on, the fluctuation in the transmitted light power diminishes.

## 5. Outlook and discussion

In the near future, things to be done include: (i) Add alignment control in the rest 3 d.o.f.'s and refine the control; (ii) Increase the finesse of the FPI; (iii) Add a polarization maintaining fiber as a simple mode cleaner [26]. Hopefully we can achieved our goal sensitivity of  $5 \times 10^{-8} \text{ rad} \cdot \text{Hz}^{-1/2}$  at 10~20 Hz. For the next phase (third phase) after this, with 5-fold improvement on optical sensitivity, 5 m rotating permanent magnet, and interferometer length extended to 7 m, vacuum birefringence would be in our reach. In this second phase, we will be able to perform an independent measurement of polarization rotation to compare with the PVLAS result [17, 21].

We would like to thank the National Science Council for supporting this work (NSC 93-2112-M-007-022, NSC 94-2112-M-007-012).

## References

- [1] Halpern O. 1933 *Phys. Rev.* **44** 855
- [2] Euler E. 1936, *Ann der Phys. (Leipzig)*, **26** 398 ; Heisenberg W. and Euler E. 1936 *Zeits. Fur Phys.* **98** 714
- [3] Bialynicka-Birula Z. and Bialynicki-Birula I. 1970 *Phys. Rev. D* **2** 2341
- [4] Adler S. L. 1971 *Ann. Phys. (USA)* **87** 599
- [5] Iacopini E and Zavattini E 1979 *Phys. Lett. B* **85** 151
- [6] Ni W-T, Tsubono K, Mio N, Narihara K, Chen S-C, King S-K and Pan S-S 1991 *Mod. Phys. Lett. A* **6** 3671
- [7] Cameron R *et al* 1993 *Phys. Rev. D* **47** 3707
- [8] Ni W-T 1974 *Bull. Amer. Phys. Soc.* **19** 655
- [9] Ni W-T 1977 *Phys. Rev. Lett.* **38** 301

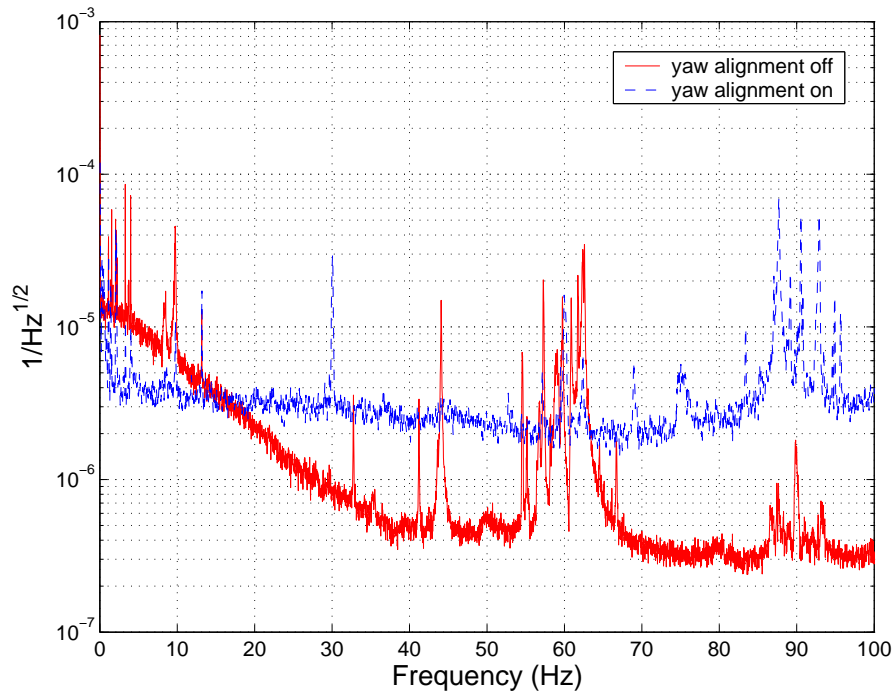


Figure 6. Ellipticity noise floor.

- [10] Ni W-T 1973 A Nonmetric Theory of Gravity (Montana State University, Bozeman, Montana, USA), preprint. The paper is available via <http://gravity5.phys.nthu.edu.tw/webpage/article4/index.html>.
- [11] Sikivie P. 1983 *Phys. Rev. Lett.* **51** 1415; Anselm A. A. 1985 *Yad. Fiz.* **42** 1480; Gasperini M. 1987 *Phys. Rev. Lett.* **59** 396
- [12] Maiani L., Petronzio R. and Zavattini E. 1986 *Phys. Lett. B* **175** 359
- [13] Raffelt G. and Stodolsky L. 1988 *Phys. Rev. D* **37** 1237
- [14] Pengo R. *et al* 1998 *Frontier Test of QED and Physics of the Vacuum* 59, ed. E Zavattini *et al* (Sofia: Heron Press); and references there in.
- [15] Nezrick F. 1998 *Frontier Tests of QED and Physics of Vacuum* 71, ed. E Zavattini *et al* (Sofia: Heron Press); and reference there in.
- [16] Ni W-T 1998 *Frontier Tests of QED and Physics of Vacuum* 83, ed. E Zavattini *et al* (Sofia: Heron Press); and reference there in.
- [17] Cantatore G. *et al* talk on QED-2005 <http://arachne.spectro.jussieu.fr/QED2005/Talks/Cantatore.pdf>
- [18] Rizzo C. *et al* talk on QED-2005 [http://arachne.spectro.jussieu.fr/QED2005/Talks/Robilliard\\_Rizzo.pdf](http://arachne.spectro.jussieu.fr/QED2005/Talks/Robilliard_Rizzo.pdf)
- [19] Chen S-J *et al* talk on QED-2005 <http://arachne.spectro.jussieu.fr/QED2005/Talks/Chen.pdf>
- [20] Chen S-J, Mei S-H and Ni W-T 2003 *Preprint hep-ex/0308071*
- [21] Cantatore G. *et al* 2005 *Preprint hep-ex/0507107*
- [22] Wu J-S, Ni W-T and Chen S-J 2004 *Class. Quant. Grav.* **21** S1259 (*Preprint physics/0308080*)
- [23] Tatsumi D, Barton M A, Uchiyama T and Kuroda K 1999 *Rev. Sci. Instrum.* **70** 1561; and references therein
- [24] Morrison E, Beers B J, Robertson D I and Ward H 1994 *Appl. Opt.* **33** 5037, 5041
- [25] Heinzel G. Ph.D. Thesis, University of Hannover 1999; MPQ Report 243 Feb. 1999
- [26] Mei H-H *et al* 2005 presented in the 6th Edoardo Amaldi Conference on Gravitational Waves, June, 2005 (Okinawa, Japan) (*Preprint physics/0508153*)